PAPER • **OPEN ACCESS**

Polycarbonate multi-wall panels integrated in multi-layer solar façade concepts

To cite this article: M ekon and K Struhala 2018 *IOP Conf. Ser.: Mater. Sci. Eng.* **415** 012019

IOP Conf. Series: Materials Science and Engineering **415** (2018) 012019 doi:10.1088/1757-899X/415/1/012019

Polycarbonate multi-wall panels integrated in multi-layer solar façade concepts

M Čekon[1] and K Struhala[1]

[1] Centre AdMaS, Faculty of Civil Engineering, Brno University of Technology, Czechia

cekon.m@fce.vutbr.cz

Abstract. Recent technological advances in transparent insulation materials´ (TIMs) production may have opened ways for new integration of these materials in buildings. This paper presents a study analysing several variants of façades incorporating TIMs on solar façade principles. The analysis is based on ongoing long-term full-scale experiments in Brno, Czech Republic. The paper introduces the test platform which is used for evaluation of specific aspects of integrated polycarbonate TIMs. The paper describes the experiment results, especially long-term thermal response and passive solar gain data. These data are applied for analysis of: influence of various polycarbonate-based TIMs on the real performance of the façades; influence of implementation of different solar absorbers on the performance of the proposed facades; effectivity of application of latent thermal energy storage (based on PCMs) as a part of heat accumulation layer and coupling of TIM with prismatic glass to enhance optical selectivity aspect. Presented results demonstrate for example significant influence of the type of solar absorber on the thermal performance of tested solar facades: the difference is up to 35% to 54%. Also the integration of prismatic glass coupled with simple two-wall polycarbonate panel can reduce solar penetration through components at the level comparable with the most complex six-wall panel.

1. Introduction

Commonly, the efficient way to improve energy consumption of buildings is based on reduction of the heating and ventilation energy losses. This can be achieved through addition of thermal insulation on the building envelope and installation of efficient HVAC system with heat recovery [1, 2]. However the potential for further savings in future building designs is limited by increasing investment costs, embodied energy and other environmental impact [3, 4, 5]. Therefore the building sector is looking for solutions that would not only minimize the energy losses [6], but also utilize the energy gains available on-site. These solutions integrate renewable energy sources (RES) such as photovoltaics (PV) or solar thermal collectors for on-site energy generation [7, 8, 9]. Although the field of RES is already well covered in literature, there are still some directions that need to be carefully investigated. Therefore this paper focuses on one of more straightforward ways for exploitation of available renewable energy gains: solar (heat) energy gains through TIMs based on Polycarbonate multi-wall panels integrated in building envelopes, particularly in multi-layer solar façade.

Integration of TIMs is already proven in case of solar thermal collectors [10, 11]. Existing TIMs [12] could be also integrated into solar thermal facades providing both transparency and thermal insulation. Several studies in the last two decades for example applied TIMs as replacement of the original glazing elements in solar wall concepts [13]. However, their involvement in building envelope is so specific that application in contemporary building practice is rather rare, even though commercial products already exist [14]. One of the main drawbacks is that specialized TIMs are rather expensive. Therefore application of cheaper materials with similar properties (such as polycarbonate sheets and

panels) is studied. Various types of multiwall panels with improved thermal properties (with optical efficiency remaining the same) are being developed. Their application in building envelopes (facades or roofs) can provide cost-effective way for achieving passive energy gains in building design [15].
This paper introduces eight experimental polycarbonate solar façade (PSF) concepts utilizing different types of TIMs (based on multiwall co-extruded polycarbonate). Components representing these PSFs are investigated as a part of long-term experiment in Brno, Czechia. Especially the influence of varying structure of TIMs (and related thermal and optical parameters) on the performance of the components is studied in detail. However, other issues like selection of proper solar absorber or incorporation of phase-change materials (PCMs) for better heat accumulation are also investigated. The paper presents comparative analysis of thermal, optical and solar properties of individual materials and illustrates performance of the whole PSF concepts on selected summer and winter days (with clear sky) measurements.

2. Experimental polycarbonate solar façade concepts

At first the properties of materials applied in the proposed concepts were tested. This was followed by full-scale testing of eight experimental PSF components in real climate conditions (see Figure 1). The full-scale tests are taking place at AdMaS research centre belonging to Brno University of Technology, Czechia [16]. The PSF components are based on four polycarbonate TIMs. The TIMs are installed in pairs of components opposite or next to each other. This limits the number of tested materials. On the other hand, it allows comparative measurements and increased accuracy of the experimental results. The test cell's longitudinal axis is oriented towards South-East / North-West. One of the walls with the test components is oriented to the South-East to receive as much solar radiation as possible. The other (North-Western) wall is adjacent to one of the AdMaS center's buildings. Therefore, the test components there are not exposed to the solar radiation directly. The space inside the test cell is divided into eight compensating boxes (TCBs) made of particleboard. They are constructed around individual PSF components of tested materials – four components on each side. The TCBs separate individual testing components from each other and the internal climate of the test cell to dampen the temperature amplitudes of the internal air. Internal climate in the test cell (not in the individual test boxes) is controlled by an air-conditioning unit.

Figure 1. Outside view of the test cell (left), inside view of the test cell with individual TCBs (middle), test cell cross section (right).

Eight full-scale PSF components (A to H) are long-term tested in real climate conditions. Components A to D are oriented to South-East, while components E to H are oriented to North-West. Thermal and optical performance of all components are described in sections 3 and 4, while real outdoor performance in section 5 is described only for components A to D oriented to the South-East (due to direct solar radiation). Schemes of the components are in Figures 2 and 3. Each tested component fulfils several different functions thanks to four functional layers. First layer of tested components is made of clear polycarbonate multi-wall panel in the role of TIM. All the TIMs are installed with air

cavities parallel to the longer side of the components. Components A and H integrate simple 10mm thick two-wall panel (PC10). In case of component A the PC10 panel is covered by prismatic glass pane rayWall90 to improve its overall optical performance.

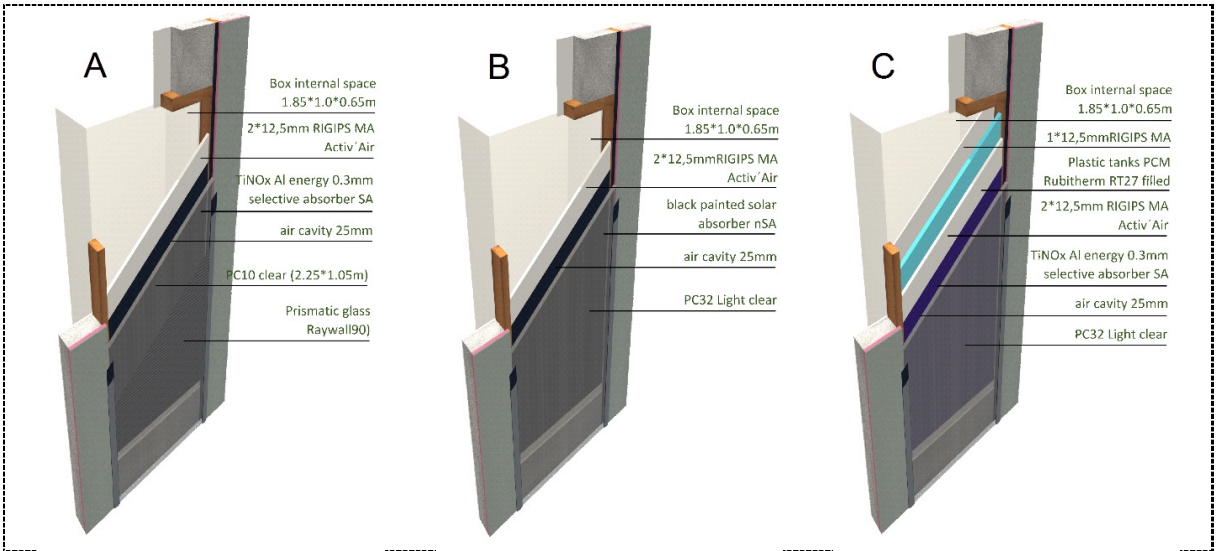

Figure 2. Test components A, B and C, key material layers, TIM and solar absorber types.

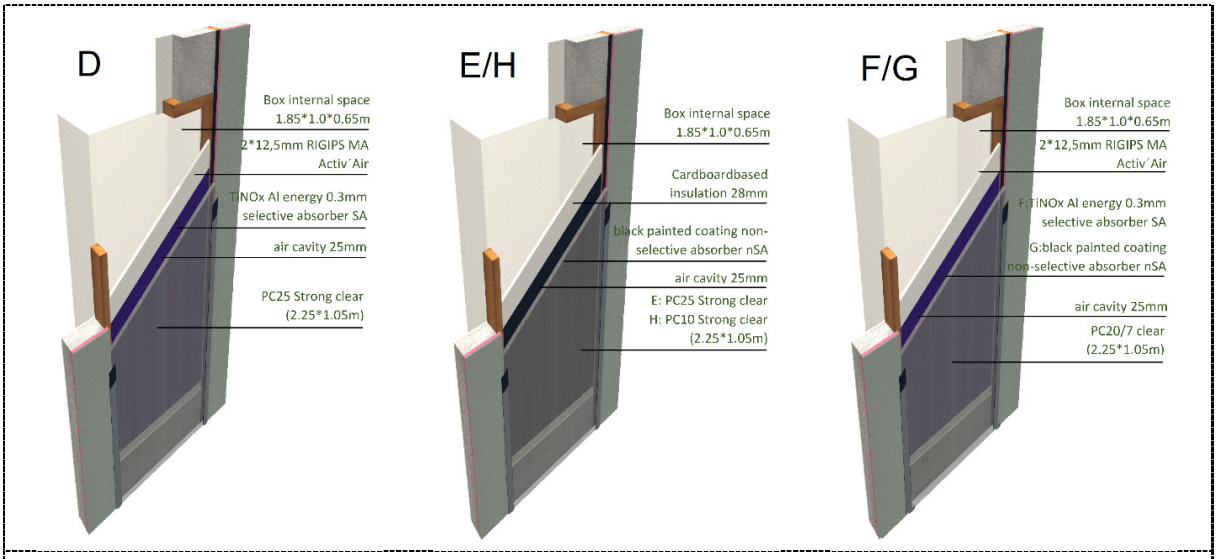

Figure 3. Test components D, E, F, G and H, key material layers, TIM and solar absorber types.

Components B and C integrate the most complex 32mm thick six-walls system with combined parallel and diagonal partitioning (PC32). Components D and E integrate 25mm thick three-wall panel with combined partitioning (PC25). Components F and G integrate 20 mm thick seven-wall panel (PC20). Basic parameters of the panels are described in Table 1. Second layer of the tested components is 25mm non-ventilated air gap. Third layer is made of a solar absorber. Two types of solar absorber are incorporated in the experimental components: selective absorber (SA) with low-e coating in components A, C, D and F and non-selective absorber (nSA) in components B, E, G and H. Reason for this is difference in the absorber's properties. The absorbers have similar solar absorbance, approx. 0.94 (SA) and 0.96 (nSA), however they significantly differ in thermal emissivity (0.06 and 0.94, respectively). Final layer of the components is the base layer for application of solar absorber. In real

façade this layer would also fulfil the role of heat accumulator. For the purpose of the described experiment this layer is simplified to a 25mm plasterboard panel in components A, B, D, F and G. 28mm corrugated fiberboard panel is incorporated in the same role in components E and H for the purpose of performance comparison. Component C is used for evaluation of PCM application. Therefore the heat accumulating layer in this component is made of Rubitherm RT27 in plastic tanks enclosed between plasterboards.

3. Thermal performance of experimental PSFs

This section presents the results of standardized calculations employed to reproduce the theoretical thermal performance of presented PSF concepts. Calculated parameters consider the influence of different thermal and optical properties. In addition, the results of the PSF concepts with and without a selective absorber are also calculated. Firstly, measured thermal conductivities of Polycarbonate multi-wall systems are presented. Secondly, the thermal parameters of the whole concepts are calculated.
Thermal properties of the TIMs were evaluated with TLP 300-DTX-1P apparatus. It utilizes guarded hot plate (GHP) method to measure heat resistance and calculate equivalent thermal conductivity in compliance with ISO 8302 [17] and EN 12667 [18]. Results of the evaluation are summed in Table 1. Temperature dependency of the thermal conductivity is taken into account as well [19].

Table 1. Key material and measured thermal parameters of evaluated polycarbonate TIMs. [19]

	PC type	*Thickness* [mm]	*Weight* [kg.m^{-2}]	*Internal cells´ structure*	Equivalent thermal conductivity at mean temperature [W·m^{-1}·K^{-1}]		
					10°C	20°C	30°C
PC10	Clear 2walls	10.3	1.7	Parallel	0.0668	0.0712	0.0763
PC20	Clear 7walls	20.7	3.0	Parallel	0.0527	0.0551	0.0582
PC25	Clear 3walls	25.1	3.4	Parallel/Diagonal	0.0665	0.0702	0.0752
PC32	Clear 6walls	32.5	3.6	Parallel/Diagonal	0.0601	0.0634	0.0684

Thermal resistances and transmittances of individual parts as well as whole experimental components were calculated according to ISO 6946 [20] using thermal conductivity values described in Table 1. Results of these calculations are summed in Table 2. The table shows values representing individual "layers" (R_t is for TIM, R_g for air gap and solar absorber, R_i heat accumulation material) or parts (R_{te} for TIM and air gap coupled with solar absorber together and their calculated equivalent thermal conductivity λ_{te}) as well as whole components (R_c). For this study, dynamic effect of phase change integrated in test component C is not considered, thus only standard calculation is provided.

Table 2. Thermal resistance for individual layers and whole components.

[m^2·K·W^{-1}]	R_t	R_g	R_i	R_{te}	λ_{te}	R_c	U_c
A	0.145	0.57	0.125	0.795	0.044	1.050	0.95
B	0.513	0.18	0.125	0.733	0.078	0.988	1.01
C	0.513	0.57	0.275	1.123	0.051	1.528	0.65
D	0.357	0.57	0.125	0.968	0.052	1.223	0.82
E	0.357	0.18	0.444	0.578	0.086	1.152	0.87
F	0.376	0.57	0.125	0.986	0.046	1.241	0.81
G	0.376	0.18	0.125	0.596	0.075	0.851	1.17
H	0.145	0.18	0.444	0.365	0.096	0.939	1.06

The different performance of both solar absorber types is clearly visible in thermal resistance R_{te} and equivalent thermal conductivity values λ_{te}. The difference in those parameters of components A and H is 54% (with PC10), B and C is 35% (PC32), D and E represents 40% (PC25) and F with G corresponds to 40% (PC20). This difference means that for example the overall *U*-value of component A (with simplest PC10 TIM) bests the *U*-value of component B (with most complex PC32 TIM).

Component B with nSA has thermal resistance of 0.988 $m^2 \cdot K \cdot W^{-1}$. Compare this with the thermal resistance of 1.528 $m^2 \cdot K \cdot W^{-1}$ of component C with the same PC32 TIM combined with SA. The equivalent thermal conductivity of all components integrating SA from 0.044 (PC10) to 0.052 (PC25) approaches to recent conventional thermal insulations (e.g. expanded polystyrene reaches the value around 0.04).

4. Optical performance of polycarbonate TIM panels

Solar transmittance of polycarbonate TIMs presented in this paper is based on previous work [19]. Table 3 presents solar transmittance values based on laboratory spectrophotometer measurements using a Perkin Lambda 1050 UV/VIS/NIR spectrophotometer with a 150mm Spectralon integrating sphere. These spectral data are registered ranging from 200 nm to 3300 nm representing all spectral regions ($\tau_{\lambda\ SRS}UV$ for ultraviolet, $\tau_{\lambda\ SRS}\ VIS$ for visible and $\tau_{\lambda\ SRS}\ NIR$ for near infrared region respectively). Each sample was measured in the centre position of vertically oriented chambers. Spectral values and integrated Total Solar Transmittance (TST - τ_{λ}) parameters from 280 nm to 2 500 nm and declared values τ_{decl} are shown as well. The lowest value represents the system PC32 with solar transmittance of 43%, while the system PC10 has transmittance of 74%. It should be noted that solar transmittance obtained by laboratory spectral measurements does not correspond with producer-declared values. The difference is more than 10%.

Table 3. Solar transmittance of tested polycarbonate TIM panels [19].

	τ_{λ} ASTM G 173 [21]	$\tau_{\lambda\ SRS}UV$ 0.2 – 0.3 µm	$\tau_{\lambda\ SRS}\ VIS$ 0.3 – 0.8 µm	$\tau_{\lambda\ SRS}\ NIR$ 0.8 – 2.5 µm	τ_{decl}
PC10	0.74	0.08	0.79	0.77	0.84
PC20	0.50	0.04	0.54	0.52	0.62
PC25	0.48	0.07	0.50	0.50	0.63
PC32	0.43	0.03	0.46	0.45	0.53

5. Real outdoor performance and thermal response

As the proposed concept is based on various solar active materials, real outdoor testing may determine the maximum temperature that can be achieved in these test solar components and thus determine their potentials. There are many specific issues to take into account, such as inclined angular dependence, fluctuations of solar irradiation, overall solar distribution or orientation to the cardinal points. These issues could be solved all together with real-life monitoring of solar thermal performance. Results of full-size experiments in real climate condition demonstrate influence of different absorber efficiencies and effect of various geometrical and physical characteristics on the performance of individual PSF components. This part of the paper focuses on components A, B, C and D oriented to the South-East to analyze the performance of the components in direct solar exposure using contact digital thermometers Maxim DS18B20. Performance of the components is analyzed during representative clear sky day (24 hours) in winter and summer, with maximum sun height above the horizon of 31° and 59° respectively. The indoor climate was not controlled during the winter day, while during summer day the indoor air temperature in the test cell was maintained approx. at 21 °C. Average outdoor air temperature was T_e = -8.63 °C in winter (24.53 °C in summer), while interior temperature was T_{ai} = 5.16 °C in winter (21.11 °C in summer). Average indoor air temperature in individual TCBs in winter (summer) day reached: T_A = 6.99 °C (27.40 °C), T_B = 8.20 °C (26.77 °C), T_C = 6.98 °C (26.16 °C) and T_D = 10.20 °C (29.36 °C). Detailed temperature measurement results are shown in Figure 4. Overall, the best efficiency (represented by the highest indoor TCB temperature) was achieved with component D. It should be highlighted that test components A and B show similar summer performance (similarly to section 3) even though their composition is significantly different. This time, the reason is likely the application of rayWall90 prismatic glass in component A, which improves summer performance of this component. It should be also noted, that winter results were influenced by the fact that indoor conditions were not controlled. This means that PCM in component

C was not fully activated and the component could not perform at peak efficiency. Therefore, the effect of C in winter is represented by more stable temperature progression comparing to those with no PCM. When looking at minimum temperatures for summer test period, test component C shows the best results due to PCM integration. Its peak indoor temperature is more than 10 K lower compared to other components.

Figure 5 presents maximum temperatures achieved on solar absorber surfaces (T_{abs}) of particular components. Interestingly, component A exhibits almost the same maximum temperatures for both winter and summer days. Component B has maximum temperatures approx. 65 °C in winter and 80 °C in summer. Here the specific optical raster applied on the model A influence the internal temperature at the level comparable with the component B. The test component C has the highest surface temperature in both winter and summer. The winter temperature is beneficial, however in summer its overall performance could cause unnecessary overheating.

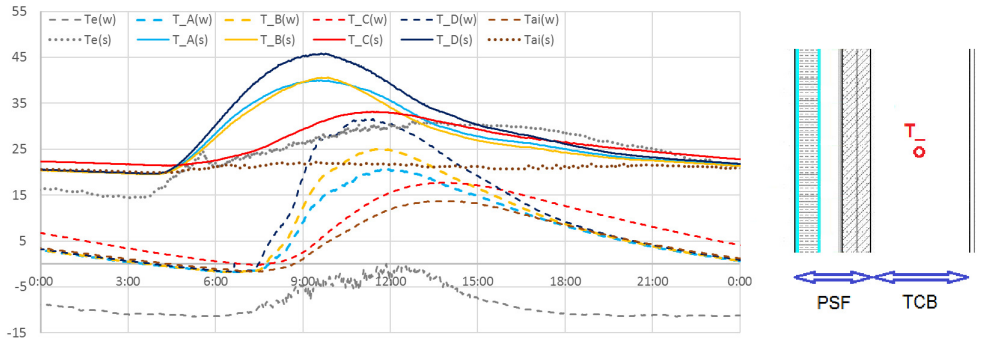

Figure 4. Internal test compensating box (TCB) temperatures; (w) winter day; (s) summer day.

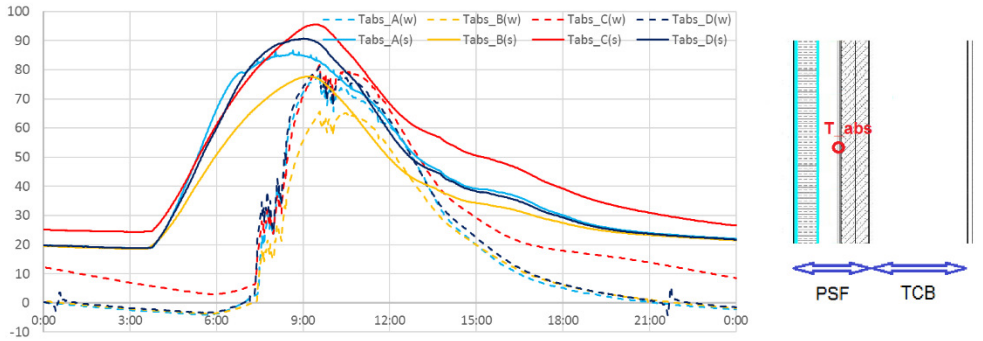

Figure 5. Absorber temperatures; (w) winter; (s) summer.

This is the reason for integration of PCM as a latent heat storage that would eliminate internal temperature fluctuations and limit the overheating. Last component D has the same absorber response in winter as C, however in summer it reaches the lower absorber temperature due to lower thermal capacity of plasterboard without PCM. Concerning only the polycarbonate TIMs, the temperature difference ΔTpc_ is a key element when temperature gradient needed to be considered for thermal calculations. Figure 6 presents results of maximum temperature difference obtained on polycarbonate systems in presented days. The maximum is achieved in winter case approaching 70K difference. When taking one particular type of PC32 into account, both test components B and C are in a strong contrast. The type of solar absorber significantly affects this aspect and the difference is almost 20K. In addition, measuring solar irradiance rates I_r and dynamic solar transmittance based on evaluating the amount of solar radiation penetrating through the multi-wall structure of the polycarbonate TIMs is provided as well (Figure 7). A specific methodical approach is applied in this relation to provide real data. During clear sky conditions, huge variation of penetrated part of solar irradiance can be

observed. Depending on the particular TIM, the values significantly vary, which influences hourly solar transmittance values. Activation of the prismatic glass integrated in A is clearly demonstrated in Figure 7, however the internal structure of C indicates the same response.

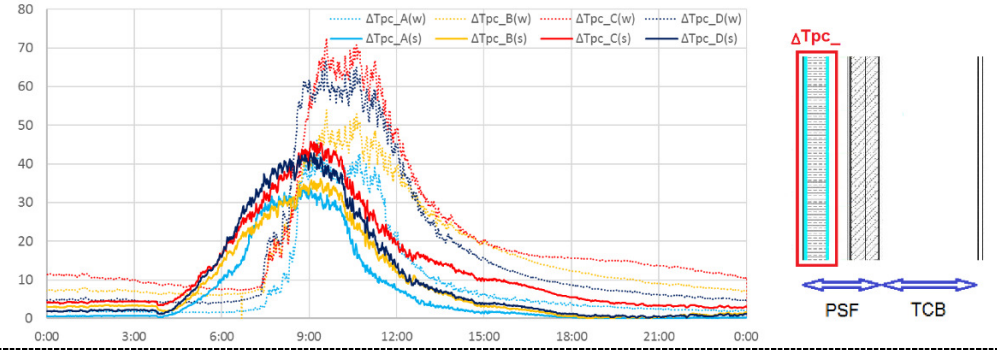

Figure 6. Temperature difference of polycarbonate systems; (w) winter; (s) summer

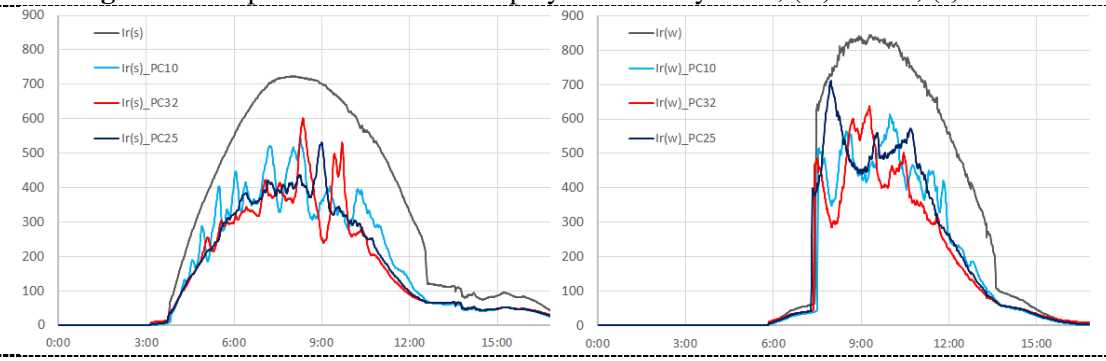

Figure 7. Solar irradiance rates penetrated through PC systems; (w) winter; (s) summer.

Conclusion

The paper presents the results of the solar and thermal characterization of proposed polycarbonate solar façade (PSF) concepts. The concepts evaluated impacts of different TIMs, selective and non-selective solar absorbers, as well as and latent thermal energy storage. Experimental monitoring of full-scale PSF components focused on the dynamic annual performance of TIMs coupled with solar absorbers as a fundamental step towards understanding overall interactions influencing the heat transfer of the presented concepts. Experimental results and calculations indicate that application of SA in proposed PSFs significantly improves their thermal parameters compared to application of nSA. Results show that when thermal resistance or equivalent thermal conductivity is considered, proposed concepts implementing the most complex PC32 TIM with SA (component C) provide comparable performance to conventional thermal insulation. When comparing the temperature response of the experimental PSF components invoked by solar radiation at its peak, a significant effect of particular solar absorber type and type of polycarbonate TIM is observed. Further research will be focused on detailed experimental analysis of long-term outdoor experiments and numerical modelling as well as the optimization of the described PSF concepts.

Acknowledgments

This research was supported by the project GJ 16-02430Y "Contemporary concepts of climatically active solar façades integrating advanced material solutions" supported by Czech Science Foundation.

References

[1] X. Liang, Z. Wang, M. Royapoor, Q. Wu, T. Roskilly (2017), Comparison of building

performance between Conventional House and Passive House in the UK, *En. Proc.* **142** 1823
[2] S. Guillén-Lambea, B. Rodríguez-Soria, J. M. Marín (2016), Review of European ventilation strategies to meet the cooling and heating demands of nearly zero energy buildings (nZEB)/Passivhaus. Comparison with the USA, *Renew Sust Energ Rev* **62** 561
[3] I. Zacà, D. D'Agostino, P. M. Congedo, C. Baglivo (2015), Assessment of cost-optimality and technical solutions in high performance multi-residential buildings in the Mediterranean area, *Energ Buildings* **102** 250
[4] T. Ekström, R. Bernardo, Å. Blomsterberg (2018), Cost-effective passive house renovation package for Swedish single-family houses from the 1960s and 1970s, *En. Buildings* **161** 89
[5] W. Ott, R. Bolliger (2015), Pitfalls in the Economic and Ecological Evaluation of Energy Related Building Renovation Strategies and Measures, *Energy Procedia* **78** 2340
[6] P. Ďurica, P. Juráš, R. Ponechal, D. Štaffenová (2016), Long-Time evaluation of thermal-Technical parameters of experimental wooden walls. In *CESB 2016 - Central Europe Towards Sustainable Building 2016*: *Innovations for Sustainable Future*, pp. 1063-1070.
[7] I. Visa, M. Moldovan, M. Comsit, M. Neagoe, A. Duta (2017), Facades Integrated Solar-thermal Collectors – Challenges and Solutions, *Energy Procedia* **112** 176
[8] R. Bolliger, W. Ott, S. von Grünigen (2015), Finding the Balance between Energy Efficiency Measures and Renewable Energy Measures in Building Renovation: An Assessment Based on Generic Calculations in 8 European Countries, *Energy Procedia* **78** 2372
[9] F. Favoino, F. Goia, M. Perino, V. Serra (2014), Experimental assessment of the energy performance of an advanced responsive multifunct. façade module, *Energ Buildings* **68** 647
[10] J. Cadafalch, R. Cònsul (2014), Detailed modelling of flat plate solar thermal collectors with honeycomb-like transparent insulation, *Solar Energy* **107** 202
[11] J. D. Osorio, A. Rivera-Alvarez, P. Girurugwiro, S. Yang, R. Hovsapian, J. C. Ordonez (2017), Integration of transparent insulation materials into solar collector devices, *Sol Energy* **147** 8
[12] N. D. Kaushika, K. Sumathy (2003) Solar transparent insulation materials: a review. *Renew Sust Energ Rev*. **7**(4) 317
[13] I. L. Wong, P. C. Eames, R. S. Perrera (2007), A review of transparent insulation systems and the evaluation of payback period for building applications, *Solar Energy* **81** 1058
[14] M. Casini (2016), Smart Buildings: Advanced Materials and Nanotechnology to Improve Energy-Efficiency and Environmental Performance, Elsevier: Cambridge, 2016, 363 p.
[15] E. Moretti, M. Zinzi, E. Belloni (2014) Polycarbonate panels for buildings: Experimental investigation of thermal and optical performance, *En Buildings* **70** 23
[16] M. Čekon, R. Slávik, K. Struhala, M. Formánek (2017) Experimental Full-Scale Test Cell Optimizing for Research of Novel Concepts towards Climatically Active Solar Façade Design, *Applied Mechanics and Materials* **861** 213
[17] ISO (1991), *Thermal insulation - Determination of steady-state thermal resistance and related properties - Guarded hot plate apparatus*, ISO 8302, International Organization for Standardization (ISO): Geneva, 1991, 47 p.
[18] ČSN EN (2001) *Thermal perforance of building materials and products – Deterination of thermal resistance by means of guarded hot plate and heat flow method*, ČSN EN 12667, Czech normalization institute (CNI): Prague, 2001, 60 p.
[19] M. Čekon, R. Slávik, J.Zach (2017) Experimental Analysis of Transparent Insulation Based on Polycarbonate Multi-Wall Systems: Thermal and Optical Performance, *Energy Procedia* **132** 502
[20] ISO (2017), *Building components and building elements — Thermal resistance and thermal transmittance — Calculation method*, ISO 6946, International Organization for Standardization (ISO): Geneva, 2017, 40 p.
[21] ASTM (2012), *Standard Tables for Reference Solar Spectral Irradiances: Direct Normal and Hemispherical on 37_ Tilted Surface;* ASTM G173-03*;* American Society for Testing and Materials (ASTM): West Conshohocken, PA, USA, 2012.